Development 126, 2631-2642 (1999)
Printed in Great Britain © The Company of Biologists Limited 1999
DEV4166

The mammalian Tolloid-like 1 gene, *Tll1*, is necessary for normal septation and positioning of the heart

Timothy G. Clark[1], Simon J. Conway[2], Ian C. Scott[1], Patricia A. Labosky[3,‡], Glenn Winnier[3], Justin Bundy[2], Brigid L. M. Hogan[3] and Daniel S. Greenspan[1,*]

[1]Department of Pathology and Laboratory Medicine and Cardiovascular Research Center, University of Wisconsin, 1300 University Avenue, Madison, WI 53706, USA
[2]Institute of Molecular Medicine and Genetics, Medical College of Georgia, 1120 15th Street, Augusta, GA 30912, USA
[3]Howard Hughes Medical Institute and Department of Cell Biology, Vanderbilt University Medical School, Nashville, TN 37232-2175, USA
[‡]Present address: Department of Cell and Developmental Biology, University of Pennsylvania, Philadelphia, PA 19104, USA
*Author for correspondence (e-mail: dsgreens@facstaff.wisc.edu)

Accepted 31 March; published on WWW 19 May 1999

SUMMARY

Mammalian Tolloid-like 1 (mTLL-1) is an astacin-like metalloprotease, highly similar in domain structure to the morphogenetically important proteases bone morphogenetic protein-1 (BMP-1) and *Drosophila* Tolloid. To investigate possible roles for mTLL-1 in mammalian development, we have used gene targeting in ES cells to produce mice with a disrupted allele for the corresponding gene, *Tll1*. Homozygous mutants were embryonic lethal, with death at mid-gestation from cardiac failure and a unique constellation of developmental defects that were apparently confined solely to the heart. Constant features were incomplete formation of the muscular interventricular septum and an abnormal and novel positioning of the heart and aorta. Consistent with roles in cardiac development, *Tll1* expression was specific to precardiac tissue and endocardium in 7.5 and 8.5 days p.c. embryos, respectively. *Tll1* expression was also high in the developing interventricular septum, where expression of the BMP-1 gene, *Bmp1*, was not observed. Cardiac structures that were not affected in *Tll1*$^{-/-}$ embryos either showed no *Tll1* expression (atrio-ventricular cushions) or showed overlapping expression of *Tll1* and *Bmp1* (aortico-pulmonary septum), suggesting that products of the *Bmp1* gene may be capable of functionally substituting for mTLL-1 at sites in which they are co-expressed. Together, the various data show that mTLL-1 plays multiple roles in formation of the mammalian heart and is essential for formation of the interventricular septum.

Key words: Astacin metalloprotease, Heart morphogenesis, Interventricular septum, Organogenesis, Mouse

INTRODUCTION

Mammalian tolloid-like 1 (mTLL-1) belongs to a group of structurally related proteases of which bone morphogenetic protein-1 (BMP-1) is the prototype. BMP-1, first identified in osteogenic extracts of bone (Wozney et al., 1988), was subsequently found to share domain structure with a small family of putative proteases implicated in embryonic patterning in diverse species (Bond and Beynon, 1995). Each member of this family contains an astacin-like protease domain and varying numbers of CUB protein-protein interaction domains and EGF motifs. Within this group BMP-1 was structurally most similar to the *Drosophila* protein Tolloid (TLD) (Shimell et al., 1991), although TLD contained additional C-terminal EGF and CUB domains. A single mammalian gene is now known to produce alternatively spliced mRNAs for BMP-1 and for a larger protein designated mammalian Tolloid (mTLD), due to a domain structure identical to that of TLD (Takahara et al., 1994).

Recently, BMP-1/TLD-like proteases, Xolloid (Piccolo et al., 1997), in *Xenopus*, and zebrafish 'Tolloid' (Blader et al., 1997) were shown to exert ventralizing effects on embryo morphogenesis through cleavage of the protein Chordin, which can form latent complexes with TGFβ-like molecules BMP-2, BMP-4, and BMP4/7 heterodimers. Similarly, TLD was shown to act in the dorsal-ventral patterning of *Drosophila* embryos by cleaving the Chordin homologue Short Gastrulation (SOG) (Marqués et al., 1997), which has been shown capable of forming latent complexes with BMP-2/4 homologue decapentaplegic (DPP) and with BMP-5/6/7 homologue screw (SCW) (Neul and Ferguson, 1998; Nguyen et al., 1998). Because BMP-1 co-purifies from osteogenic bone extracts with BMPs -2 through -7 (Wozney et al., 1988; Celeste et al., 1990), and because overexpression of BMP-1 can ventralize *Xenopus* embryos (Goodman et al., 1998), it has been suggested that BMP-1 may also affect morphogenesis by augmenting the activities of TGFβ-like BMPs.

BMP-1 and mTLD affect morphogenetic processes, at least

in part, through multiple effects on matrix deposition. These include provision of procollagen C-proteinase activity, which cleaves the C-propeptides of procollagens I-III (Kessler et al., 1996; Li et al., 1996); and the proteolytic activation of lysyl oxidase (Panchenko et al., 1996), an enzyme necessary to formation of covalent cross-links in collagen and elastic fibers. However, despite the multiple functions of the *Bmp1* gene, homozygous null mutant embryos, though perinatal lethal, lack gross defects in patterning or skeletogenesis (Suzuki et al., 1996). This suggested genetic redundancy and has led to isolation of cDNAs encoding two genetically distinct proteins designated mammalian Tolloid-like 1 (mTLL-1) (Takahara et al., 1996), and mammalian Tolloid-like 2 (mTLL-2) (I. C. Scott, I. L. Blitz, W. N. Pappano, Y. Imamura, T. G. C., B. M. Steiglitz, C. L. Thomas, S. A. Maas, K. W. Y. Cho and D. S. G., unpublished data) due to domain structures and sequences highly similar to those of mTLD.

It has been suggested that mTLL-1 is the mammalian homologue of Xolloid and TLD (Marqués et al., 1997; Piccolo et al., 1997) and/or that it provides procollagen C-proteinase activity that partially compensates for loss of BMP-1 and mTLD in *Bmp1*-null mice (Takahara et al., 1996). To define the role of mTLL-1 in mammalian development, we have disrupted the cognate *Tll1* gene via homologous recombination in ES cells. Homozygous mutant embryos die at mid gestation, and display severe edema and congestion of blood indicative of cardiac failure. Developmental defects of $Tll1^{-/-}$ embryos appear to be limited solely to the heart or to result secondarily from heart defects. Homozygous mutant hearts show a spectrum of cardiac defects including double outlet right ventricle (DORV), double inlet left ventricle (DILV), ventricular septal defect (VSD), atrial septal defect (ASD), and a unique displacement of the heart and descending aorta from their normal positions. Of these defects, the most consistent features are the VSD and displacement in the positions of heart and aorta. Correlation of these defects with the distribution of *Tll1* expression in normal mouse development indicates that the gene for mTLL-1 is essential to normal positioning and septation of the mammalian heart.

MATERIALS AND METHODS

Construction of the targeting vector

A replacement targeting vector (see Fig. 1A) was generated by inserting genomic DNA fragments, isolated from a 129/Sv mouse λ-Fix II genomic library (Stratagene), into vector pPNT (Tybulewicz et al., 1991) in which neomycin resistance and thymidine kinase cassettes (neo^r and TK, respectively, Fig. 1A) are both driven by the strong *Pgk1* promoter. The 5′ homology region upstream of the *neo* cassette was created by inserting a 3.2 kb *Eco*RI-*Xba*I genomic fragment between the corresponding sites in pPNT. To create the 3′ homology region downstream of the *neo* cassette, a 3.6 kb genomic fragment was excised from a λ-Fix II clone by cutting an EcoRV site within the insert and a *Not*I site within the vector. This 3.6 kb piece was inserted between the *Eco*RV and *Not*I sites of pBluescript II KS^+ (Stratagene), excised as a 3.6 kb *Sal*I fragment by cutting at *Sal*I sites flanking the insert in pBluescript and remaining λ-Fix II sequences, and inserted into the *Xho*I site of the pPNT construct already containing the 5′ homology region. In the resulting targeting vector, the *neo* cassette replaces approx. 800 bp of genomic sequences including the entire *Tll1* sixth exon.

Electroporation and selection of ES cells

TL1 ES cells, used for targeting and derived from 129/SvEvTac blastocysts, were described by Labosky et al. (1997). 150 μg of targeting vector, linearized at a unique *Not*I site (Fig. 1A), was electroporated into 5.8×10^7 cells as described by Winnier et al. (1995). Cells were then plated onto neo^r primary mouse embryo fibroblasts, cultured and sequentially selected in 300 μg G418 (Gibco BRL) at 24 hours and 2×10^{-6} M gancyclovir (a kind gift from Syntex) at 72 hours, as described (Winnier et al., 1995). Genomic DNA from 113 G418/gancyclovir double-resistant clones was analyzed by Southern blot (see below) and fourteen targeted lines were identified, indicating a targeting frequency of 1 in 8.

DNA and RNA analyses

ES cell lines were analyzed by Southern blots (Church and Gilbert, 1984) of genomic DNA restricted with *Pst*I and separately hybridized to 5′ and 3′ external probes (Fig. 1A). Southern blot analysis with a *neo* probe confirmed the absence of rearrangements or random integrations (data not shown). For genotyping mice and embryos, genomic DNA was prepared from tail and yolk sac samples, as described by Hogan et al. (1994), and analyzed by Southern blots of *Pst*I-restricted DNA hybridized to the 3′ external probe, or by PCR. For PCR genotyping, reverse primer 5′-GTTCCTGGCGTAGTGC-ATGATACTGTC-3′, corresponding to sequences within *Tll1* exon VII (nucleotides 1516-1490 of the cDNA sequence; Takahara et al., 1996) and forward primer 5′-GTCACCATCATTAGAGAGAACATCCAG-3′, corresponding to sequences within *Tll1* exon VI (nucleotides 1391-1417 of the cDNA sequence) produced an approx. 3.3 kb product from the wild-type allele, and no product from the targeted allele, while the same reverse primer with neo primer 5′-CGCTGCCTCGTCCTG-CAGTTCATTCAG-3′ (Beck et al., 1982) produced an approx. 3.6 kb product from the targeted allele and no product from the wild-type allele (data not shown). The assay employed long-distance PCR conditions (Barnes, 1994) using Taq Extender PCR additive (Stratagene) and TaqStart antibody (Clontech) at 94°C/5 minutes followed by 32 cycles of 98°C/5 seconds, 68°C/3 minutes, and final extension at 72°C/10 minutes.

Tll1 RNA transcripts (Fig. 1D) were characterized by reverse transcription (RT)-PCR using primers 5′-GAAGAATTGGCTCTGG-CTTGGAGC-3′ (forward) and 5′-GAAGGTGTTCCTGGCGTAGT-GCAT-3′ (reverse) (nucleotides 957-980 and 1499-1522, respectively, of the cDNA sequence; Takahara et al., 1996). Poly(A)$^+$ RNA for RT-PCR was isolated from whole 13.5 days post coitum (dpc) embryos using a FastTrack 2.0 kit (Invitrogen). Template cDNA was prepared from RNA using SuperScript II reverse transcriptase (Gibco BRL) and PCR was performed at 95°C/2 min followed by 35 cycles of 95°C/5 seconds, 55°C/30 seconds, 72°C/2 minutes and final extension at 72°C/10 minutes. To control for use of similar amounts of RNA, RT-PCR was performed on each sample using a mouse G3PDH amplimer set (Clontech).

Generation of chimeras and mutant mice

ES cells from two independently targeted cell lines were injected into C57BL/6 blastocysts that were implanted into pseudopregnant females as described by Hogan et al. (1994). Resultant male chimeras were mated with outbred Black Swiss females (Taconic) and agouti offspring were analyzed for the targeted allele by Southern blot. Heterozygous animals were interbred to produce litters containing homozygous, heterozygous and wild-type embryos for comparative phenotypic analyses.

In situ hybridization

Tll1 expression was detected using a mixture of two antisense riboprobes, corresponding to nucleotides 4283-4681 and nucleotides 3666-4085 of the *Tll1* 3′-untranslated region, as previously described (Takahara et al., 1996). Sense versions of the *Tll1* riboprobes, for use in control in situ hybridization, were also generated as described (Takahara et al., 1996), as were antisense and sense riboprobes specific for BMP-1 or mTLD sequences. Antisense and sense *Nkx2-*

5 riboprobes were prepared corresponding to nucleotides 821-1595 of the published sequence (Lints et al, 1993). Riboprobes were synthesized following manufacturer's conditions (Stratagene) and labeled with ^{35}S-UTP (>1000 Ci/mmol; Amersham). In situ hybridizations were performed as described by Takahara et al (1994) except that tissue sections were 5 μm thick and mounted four to nine per slide. Slides were analyzed using light- and dark-field optics of a Zeiss Axiophot 2 microscope.

RT-PCR analysis of mouse heart RNA

Embryo and adult mice were dissected in ice-cold diethylpyrocarbonate-treated saline, their hearts were isolated, snap frozen, stored at −70°C and RNA was isolated from pooled hearts using TRIzol (Gibco-BRL). RT of 300 ng RNA was as previously described (Conway et al., 1997b) and amplification of the 555 bp mTLL-1 PCR product was as described above. Conditions for amplification of the 542 bp Chordin product were the same as for the mTLL-1 product, except that primers were 5′-GGATTCTATGGCTCAGAG-GCTCAGGG-3′ (forward) and 5′-TCTCCTGGCTCCAGATT-TGGTAGGCTGG-3′ (reverse) (nucleotides 1810-1835 and 2324-2351, respectively, of the murine Chordin cDNA sequence; Pappano et al., 1998). To control for variations in RNA isolation, RT efficiency and gel loading, cDNA was used for PCR amplification of an 1100 bp G3PDH product, using forward primer 5′-ACCGGATTTGGCCGTATT-3′ and reverse primer 5′-TCTGGGATGGAAATTGTGAG-3′. For each type of RT-PCR (mTLL-1, Chordin, or G3PDH) 27, 30 and 35 cycles of amplification were carried out, to ensure that products were within the linear range. Products were electrophoresed on a 1.5% agarose gel and visualized with ethidium bromide.

RESULTS

Targeting of the *Tll1* gene

Overlapping genomic clones containing *Tll1* exons II through VII were isolated from a 129/Sv library. The 179 bp exon VI was found to encode the metzincin HEXXHXXGXXH zinc-binding active site necessary for proteolytic activity (Stöcker et al., 1995) and a targeting construct (Fig. 1A) was designed to create a mutant allele in which exon VI is replaced with a *neo*^{r} gene inserted in a transcriptional orientation opposite that of the *Tll1* locus. Deletion of exon VI also causes a frame-shift, with sequences downstream of the exon V/exon VII junction encoding only 20 amino acid residues in the new frame followed by a premature stop codon. Although the mutant allele potentially produces a short truncated protein composed primarily of proregion sequences, previous studies have shown that similar truncations of TLD are null mutations (Childs and O'Connor, 1994; Finelli et al., 1994). The absence of abnormalitites in mice heterozygous for the targeted *Tll1* allele (see below) also suggests that it is essentially null.

Two ES cell lines with correctly targeted *Tll1* alleles (Fig. 1B) were separately injected into C57BL/6 blastocysts and gave rise to chimeras which transmitted the targeted allele to progeny. Heterozygotes of each line appeared grossly normal. Separate interbreeding of heterozygotes resulted in homozygotes (Fig. 1C) with a phenotype that appeared identical for the two lines. RT-PCR analysis of poly(A)$^{+}$ RNA from whole 13.5 dpc

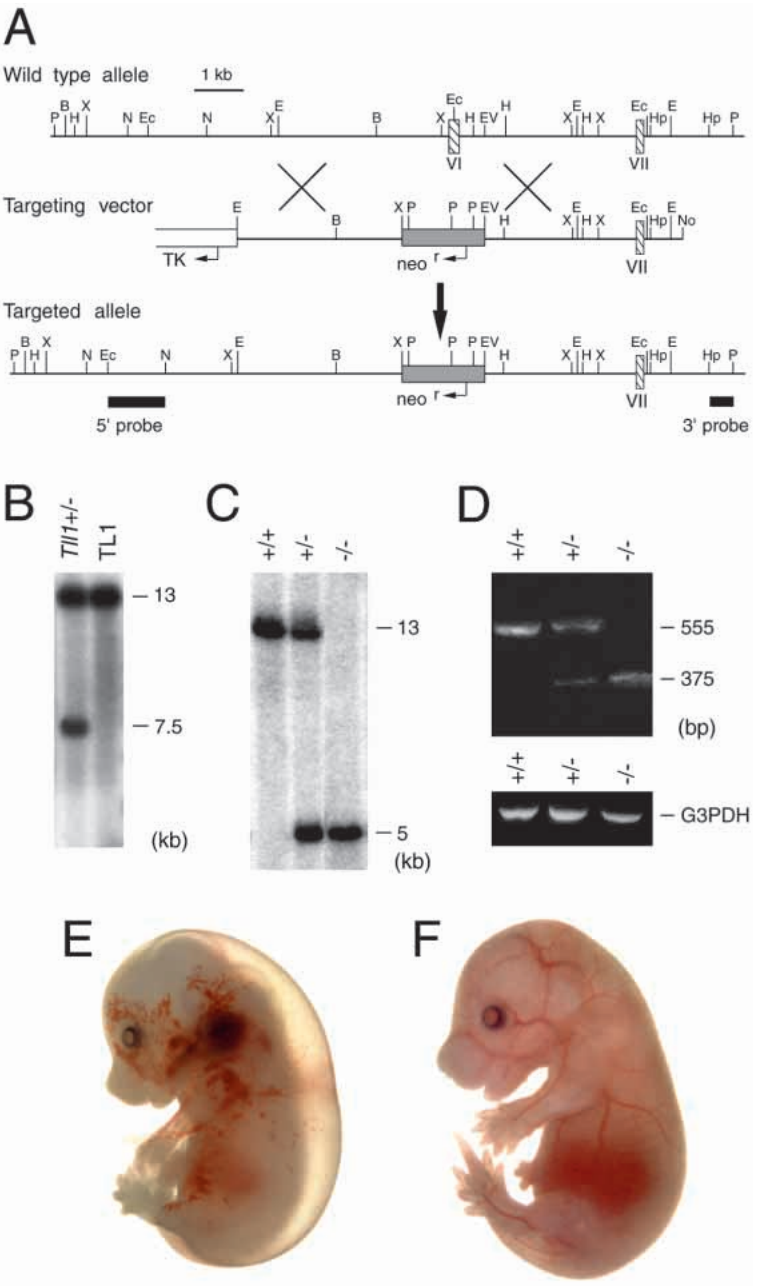

Fig. 1. Targeted disruption of *Tll1*. (A) Structure of the targeting vector and *Tll1* locus before and after homologous recombination. Arrows show the start sites and direction for transcription of the *neo* (shaded box) and *tk* (open box) cassettes. Hatched boxes represent *Tll1* exons. Black boxes represent a 1.1 kb *Eco*72I-*Nhe*I 5′ external probe and a 496 bp *Hpa*I-*Pst*I 3′ external probe. B, *Bam*HI; E, *Eco*RI; Ec, *Eco*72I; EV, *Eco*RV; H, *Hin*dIII; Hp, *Hpa*I; N, *Nhe*I; No, *Not*I; P, *Pst*I; X, *Xba*I. (B) Southern analysis of *Pst*I-restricted genomic DNA from parental (TL1) or a correctly targeted line (*Tll1*+/–) of ES cells. The 5′ probe detected approx. 7.5 and approx. 13 kb bands from the targeted and wild-type alleles, respectively. (C) Southern analysis of *Pst*I-restricted genomic DNA from yolk sacs of 11.5 dpc wild-type (+/+), heterozygous (+/–), and homozygous null (–/–) embryos. The 3′ probe detected approx. 5 and approx. 13 kb bands from targeted and wild-type alleles, respectively. (D) RT-PCR analysis of poly(A)$^{+}$ RNA prepared from whole 13.5 dpc embryos detected 555 and 375 bp products produced by wild-type and targeted alleles, respectively, and a 452 bp G3PDH product as a control (lower panel). (E) 13.5 dpc *Tll1* $^{-/-}$ (left) and +/+ (right) littermates.

embryos confirmed that only *Tll1* transcripts with the expected deletion were produced in *Tll1*$^{-/-}$ animals (Fig. 1D).

Phenotypes of *Tll1*$^{-/-}$ embryos

Of over 300 genotyped pups from –/+ to –/+ matings, none were *Tll1*$^{-/-}$, indicating embryonic lethality for homozygous null animals. Examination of over 500 genotyped embryos from 10.5 to 18.5 dpc (Table 1) showed that a distinctive phenotype associated with *Tll1*$^{-/-}$ embryos appeared at 13.5 dpc and that the majority of *Tll1*$^{-/-}$ embryos died between 14.5 and 16.5 dpc. At the time of death, the majority of *Tll1*$^{-/-}$ embryos exhibited marked edema, pallor, congestion of blood and an absence of clearly visible vasculature due to a paucity of blood in the cardiovascular system (Fig. 1E). These signs are indicative of cardiac failure (Conway et al., 1997a). Indeed, further examination of *Tll1*$^{-/-}$ embryos revealed a unique phenotype with observable defects that seemed wholly confined to the heart or to have resulted secondarily from cardiac failure (e.g. damage to dermis and underlying mesenchyme from edema).

Histological analysis of sixteen 13.5 dpc *Tll1*$^{-/-}$ mutant embryos showed that each had a large interventricular septal defect beneath the superior bridging leaflet (Fig. 2F). Moreover, 12 of the 16 embryos had a balanced atrio-ventricular septal defect with divided orifices (Fig. 2G), showing abnormal septation of both the ventricles and atria. Associated with the atrio-ventricular septal defect, dysplasia of the mitral valve was observed in 8/16 13.5 dpc *Tll1*$^{-/-}$ embryos. Consistent with the condition of cardiac failure, cardinal veins were fluid-filled and the fetal liver was engorged with blood (Fig. 2D,F,H). An interesting and unique finding, in 16/16 embryos, was abnormal positioning of the descending aorta in the center of the embryo (Fig. 2D,E,G,H,I) and shifting of the entire mutant heart towards the left side of the embryo (Fig. 2E). In 5/16 13.5 dpc *Tll1*$^{-/-}$ embryos, both the normally divided aorta and pulmonary trunk exited the right ventricle, resulting in the heart defect, double-outlet right ventricle (Fig. 2F). In one of the 13.5 dpc *Tll1*$^{-/-}$ embryos, double-inlet left ventricle, in which both atria open into the left ventricle, was also observed (data not shown). Septation of the common outflow tract into the separate aorta

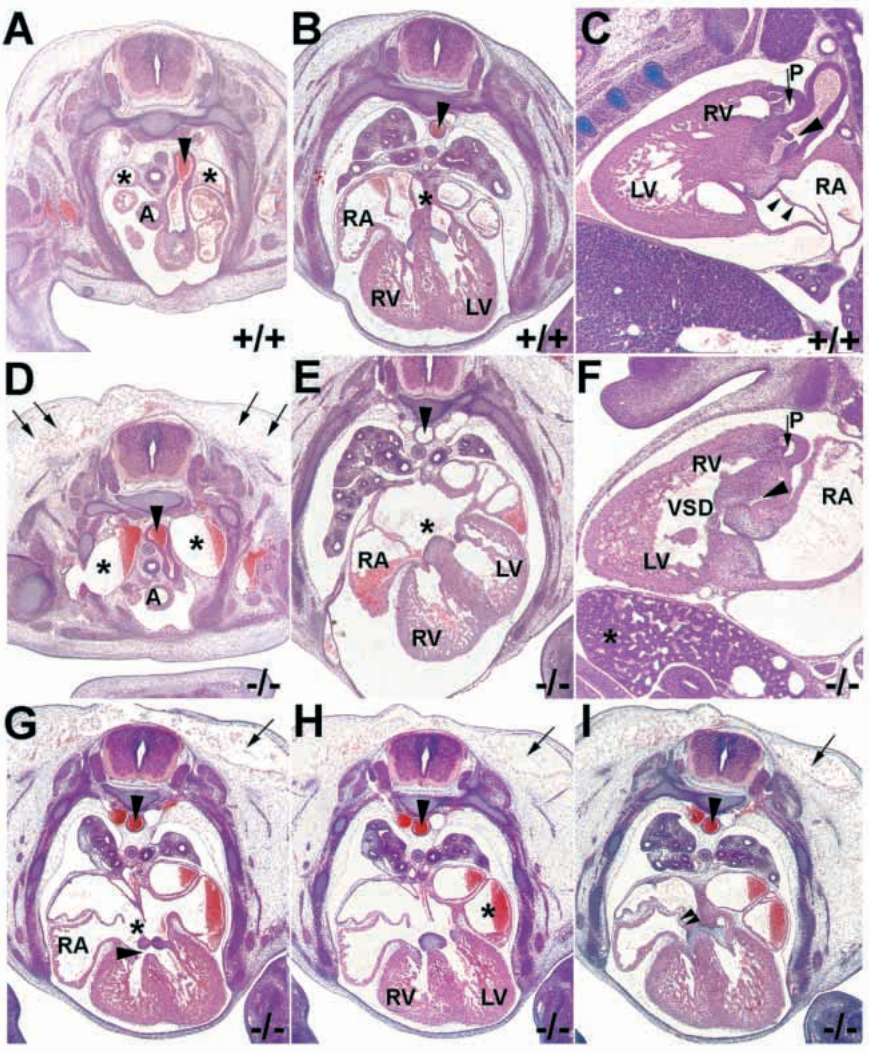

Fig. 2. Histological examination of cardiac abnormalities in *Tll1*$^{-/-}$ 13.5 dpc embryos by hematoxylin and eosin staining. A and B are transverse sections and C is a sagittal section of a normal embryo. D-I are transverse sections of *Tll1*$^{-/-}$ embryos (except F which is a sagittal section). There is a separate aorta and pulmonary trunk, with the pulmonary trunk connected to the descending (thoracic) aorta via the ductus arteriosus in both normal (A) and *Tll1*$^{-/-}$ (D) embryos. However, the descending aorta is abnormally positioned in the center of the mutant embryo (large arrowhead in D,E,G,H,I), rather than in its normal position towards the left of the trachea (large arrowhead in A,B). Also, the mutant embryo (D) is severely edematous (arrows) and the cardinal veins are dilated and blood filled (compare * in A and D). The four heart chambers are connected appropriately, but the entire mutant heart (E) is shifted to the left of the embryo (compare B and E). In addition, there is complete absence of the normal atrial septum (compare * in B and E). In the sagittal sections, the atrial septum (small arrowheads in normal embryo in C) is absent in the *Tll1*$^{-/-}$ embryo (F), but the base of the atrial septum is preserved. There is a large opening between the left and right ventricles due to absence of the muscular interventricular septum (MIVS), resulting in a ventricular septal defect, and both vessels exit from the right ventricle (F). Also, both the aortic (large arrowhead) and pulmonary (arrow) semilunar valves are severely dysplastic in this mutant (F) and the fetal liver is engorged with blood (* in F). (G,H,I) Serial sections through a single mutant embryo, illustrating the spectrum of cardiac abnormalities present in *Tll1*$^{-/-}$ embryos. This mutant has a balanced atrio-ventricular septal defect (* in G) with a common atrio-ventricular junction, but with an interventricular defect (arrowhead in G) beneath the superior bridging leaflet. The central mesenchymal mass is suspended between the lower edge of the atrial septum and there is a gap between it and the MIVS. The valvar leaflets are attached to the crest of the ventricular septum and the left superior caval vein is grossly enlarged (* in H) indicating that this mutant is severely edematous (arrow). The venous valves are attached to the spina vestibuli (small arrowheads in I). A, proximal part of arch of aorta; RV, right ventricle; LV, left ventricle; RA, right atria; P, pulmonary trunk; VSD, interventricular septal defect.

Table 1. Phenotypes and genotypes observed during gestation

Days p.c.	Total embryos (including resorbed)	Genotypes of all embryos*			Embryos with abnormal phenotype‡			Non-genotyped/ resorbed
		+/+	+/–	–/–	+/+	+/–	–/–	
10.5	48	11 [1]	28	5 [1]	0	0	0	2
11.5	34	8	13	11	0	0	0	2
12.5	40	6 [1]	17 [3]	6 [1]	0	0	0	6
13.5	165	39 [1]	72 [1]	38 [1]	0	0	17	13
14.5	114	36 [2]	49 [1]	13 [5]	0	0	14	8
15.5	98	27	45 [1]	2 [11]	0	0	13	12
16.5	52	11	34	0 [3]	0	0	3	4
17.5	25	5	12	0	0	0	0	8
18.5	5	3	2	0	0	0	0	0
Totals	581	146 [5]	272 [6]	75 [22]	0	0	47	55

*Bracketed numbers represent dead genotyped embryos.

‡Abnormal phenotype here refers to embryos that showed the full-blown syndrome of pronounced edema, pallor and congestion of blood, upon gross examination. Additional –/– embryos showed varying degrees of edema and showed cardiac defects upon histological examination.

and pulmonary trunk appeared unaffected, as all 16 mutants had a separate aorta and pulmonary trunk. However, perhaps as a result of misalignment, semilunar valves were severely dysplastic in some mutants (Fig. 2F), the valvar leaflets were attached to the crest of the ventricular septum (Fig. 2H), and the venous valves were attached to the spina vestibuli (Fig. 2I).

In all 13.5 dpc *Tll1*$^{-/-}$ embryos, the myocardium appeared unaffected, and the endocardial cushions were present and yielded normal atrio-ventricular valves. However, the endocardial ridges failed to form properly and fuse to develop functional semilunar valves (Fig. 2F). This failure to maintain a uni-directional blood flow, combined with the failure to septate the common ventricular chamber (ventricular septal defects are left-to-right shunts that place a burden on the right side of the heart), resulted in hemodynamic overload, eventually leading to cardiac failure and embryonic lethality.

To determine the initial abnormality that gives rise to the spectrum of cardiac abnormalities observed in 13.5 dpc *Tll1*$^{-/-}$ embryos, histological analysis of developmentally younger *Tll1*$^{-/-}$ embryos was carried out. The first phenotypic cardiac abnormality was observed in 11.0 dpc mutant embryos. In five *Tll1*$^{-/-}$ 11.0 dpc embryos examined, the paired dorsal aorta and cardinal veins already showed signs of cardiac failure, as they were blood-filled and dilated (Fig. 3C,D). Additionally, there was an abnormally large opening between the future left and right atria, due to the absence of a normal septum primum (Fig. 3D). Similarly, the muscular interventricular septum (MIVS) had failed to elevate, resulting in an abnormally large opening between the future left and right ventricles (Fig. 3D).

Spaciotemporal expression pattern of *Tll1* in mouse heart

To correlate *Tll1* expression with the phenotype of *Tll1*$^{-/-}$ embryos, a series of in situ hybridizations was performed analyzing the spaciotemporal expression of *Tll1* in normal developing mouse hearts. Analysis of *Tll1* expression began with examination of 7.5 dpc embryos of the late allantoic bud stage, as defined by Downs and Davies (1993). At this stage, punctate *Tll1* signal was localized to the anterior portion of the embryo, distributed symmetrically to either side of the neural groove in precardiac mesoderm (Fig. 4A). Hybridization of serial sections of the same embryo to probes for *Tll1* and for the cardiac-specific transcription factor Nkx-2.5 (Komuro and Izumo, 1993; Lints et al., 1993) confirmed that expression of

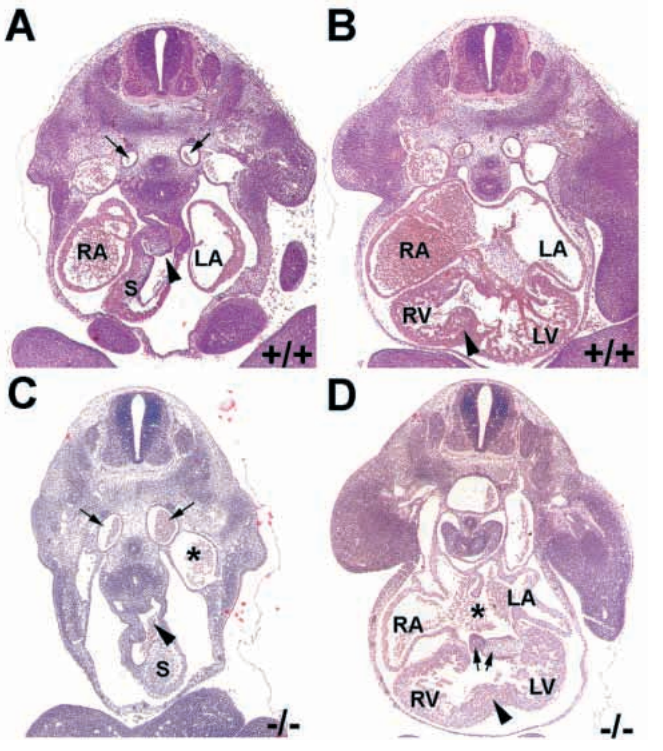

Fig. 3. Histological examination of cardiac abnormalities in *Tll1*$^{-/-}$ 11.0 dpc embryos by hematoxylin and eosin staining. (A,C) Transverse sections through the outflow tract region of normal (A) and *Tll1*$^{-/-}$ (C) embryos. The left cardinal vein (*) and the paired dorsal aorta (black arrows) are dilated, and the aortic sac (arrowhead) is shifted to the left in the mutant embryo. Both bulbar ridges (endocardial cushions) of the outflow tract septum are present in normal (A) and *Tll1*$^{-/-}$ (C) embryos. (B,D) Transverse sections through the ventricles of normal (B) and *Tll1*$^{-/-}$ (D) embryos. Cardinal veins are dilated in the mutant embryo (D), and there is a large opening between the left and right atria due to absence of the septum primum (*). Also, the muscular ventricular septum has failed to rise (arrowhead) and there are two un-fused endocardial cushions (arrows) in the atrio-ventricular canal of the *Tll1*$^{-/-}$ embryo (D). RV, right ventricle; LV, left ventricle; RA, right atria; LA, left atria; S, future aortico-pulmonary spiral septum.

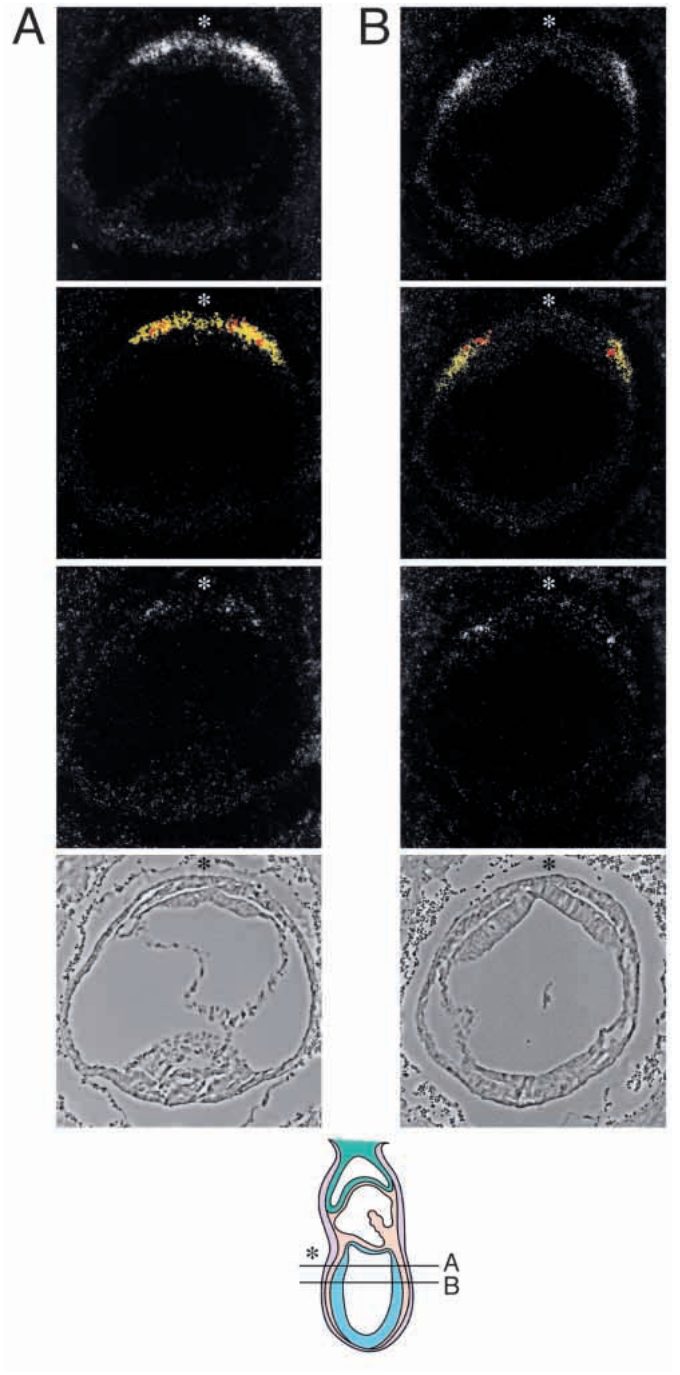

Fig. 4. Expression of *Tll1* and *Nkx2-5* in 7.5 dpc embryos. Dark-field photomicrographs are shown for in situ hybridization of an *Nkx2-5* antisense probe (top row), and dark-field (third row) and corresponding bright-field (fourth row) photomicrographs are shown for in situ hybridization of a *Tll1* antisense probe. Sections in the same column (A or B) are adjacent serial sections. The regions from which the two pairs of serial sections were taken are shown in a drawing of a late allantoic bud embryo (bottom). For each pair of serial sections, *Tll1* and *Nkx2-5* signals were colorized (red and yellow, respectively) and the corresponding serial sections were superimposed using Adobe Illustrator, to demonstrate overlap of *Tll1* and *Nkx2-5* signals (second row). Asterisks denote the anterior of the embryo.

Tll1 occurred within the expression domain of the *Nkx2-5* gene (Fig. 4A-C) and, thus, within tissue of cardiac lineage.

At 8.5-9.0 dpc, embryonic expression of *Tll1* was largely localized to the endocardial layer of the heart tube, with high levels of transcripts in the endocardial lining of the common atrial chamber (Fig. 5A,B). High levels of *Tll1* expression were also observed in the endocardial lining of the left and right horns of the sinus venosus (Fig. 5C,D), but *Tll1* expression was not detected in the endocardial lining of the bulbus cordis region of the primitive outflow tract (data not shown). Extraembryonic *Tll1* expression was also observed, localized in the blood islands associated with extraembryonic membranes (Fig. 5A,B).

At 9.5 dpc (Fig. 5E,F), *Tll1* is strongly expressed in the midline dorsal aorta and umbilical veins of the embryo. Of special note, *Tll1* is also localized in the endocardial lining of the common atrial chamber overlying the dorsal mesocardium. This is the future site where an epithelial to mesenchymal transformation will occur in the roof of the atria to give rise to the atrial septum. Of equal note, *Tll1* is expressed in the inferior myocardial wall of the common ventricular chamber at the site of the formation of the future MIVS.

At 10.5 dpc there is continued strong expression in the midline dorsal aorta, and in the cardinal and umbilical veins of the embryo (Fig. 6A,B). In addition, *Tll1* is now expressed in both the inferior and superior myocardial walls of the common ventricular chamber at the site of the future MIVS (Fig. 6C,D). However, the highest level of expression in the embryonic heart is seen in the dorsal component of the septum primum (the future atrial septum), in the endocardial lining of the common atrial chamber, and in the sinus venosus (Fig. 6E,F). Beneath the sinus venosus, expression of *Tll1* is also seen within elements of the hepatic/biliary primordia within the septum transversum (Fig. 6E,F). At 10.5 dpc, some *Tll1* expression is seen within a few cells of the endocardial lining of the outflow tract (Fig. 6A,B). No *Tll1* expression was observed in the endocardial cushion tissue of the atrio-ventricular canal (data not shown).

At 11.5 dpc *Tll1* expression becomes just discernible in the cranial ridge of mesenchymatous tissue of the aortico-pulmonary spiral septum of the outflow tract of the heart (Fig. 7A,B). Expression is also found, at this time, in the endocardial cushion tissue of the aortico-pulmonary septum, but only where this tissue is juxtaposed to the surrounding myocardial cuff. Expression of *Tll1* is also evident around the 6th branchial arch artery that connects to the aortic sac of the outflow tract, in the pericardium lining the thoracic wall overlying the pericardial cavity, and in the medial nasal process (Fig. 7A,B). Interestingly, strong *Tll1* expression is seen throughout the MIVS (Fig. 7C-F), patchy signal can be seen in the septum primum (Fig. 7E,F) and a strong signal is observable in the endocardial lining of the left and right atria adjacent to the septum primum (Fig. 7G,H). Signal was not widely present in the endocardial cushion tissue of the atrio-ventricular canal (Fig. 7C,D). In the 11.5 dpc sections shown, signal is observed in the cardinal vein (Fig. 7G,H) and strong signal is seen in a sclerotomal condensation (Fig. 7G,H).

At 12.5 dpc, *Tll1* continues to be highly expressed throughout the MIVS, and is now also strongly expressed in the cranial ridge of mesenchymatous tissue of the aortico-pulmonary spiral septum of the outflow tract of the heart (Fig. 8A,B) and within the endocardial cushion tissue of the aortico-pulmonary septum (Fig. 8C,D). There is still, however, no expression in the atrio-ventricular endocardial

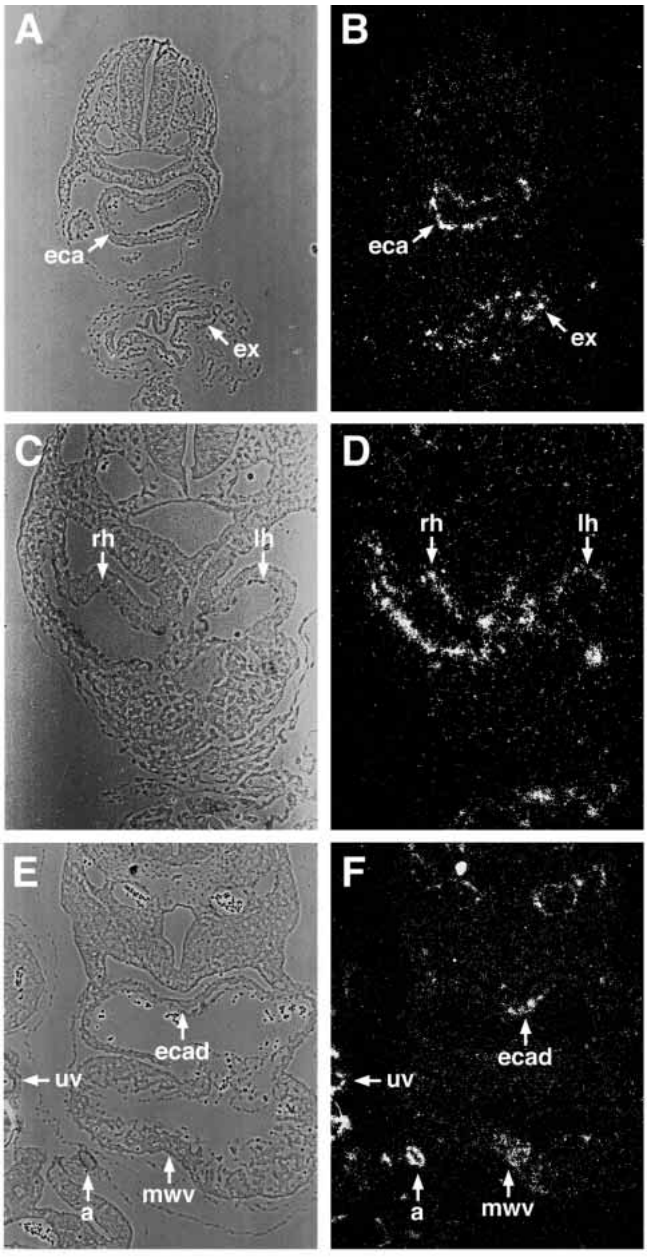

Fig. 5. Expression of *Tll1* in 8.5-9.0 and 9.5 dpc mouse embryo hearts. Bright-field (A,C,E) and corresponding dark-field (B,D,F) photomicrographs are shown for in situ hybridization of a *Tll1* antisense probe to transverse sections of an 8.5-9.0 dpc (A-D) and a 9.5 dpc (E,F) embryo. (eca, endocardial lining of common atrial chamber; ex, extraembryonic membranes and associated blood islands; lh and rh, left and right horns of the sinus venosus; a, aorta; uv, umbilical veins; ecad, endocardial lining of common atrial chamber overlying the dorsal mesocardium (future site of the atrial septum); mwv, myocardial wall of the common ventricular chamber at the site of formation of the future interventricular septum.

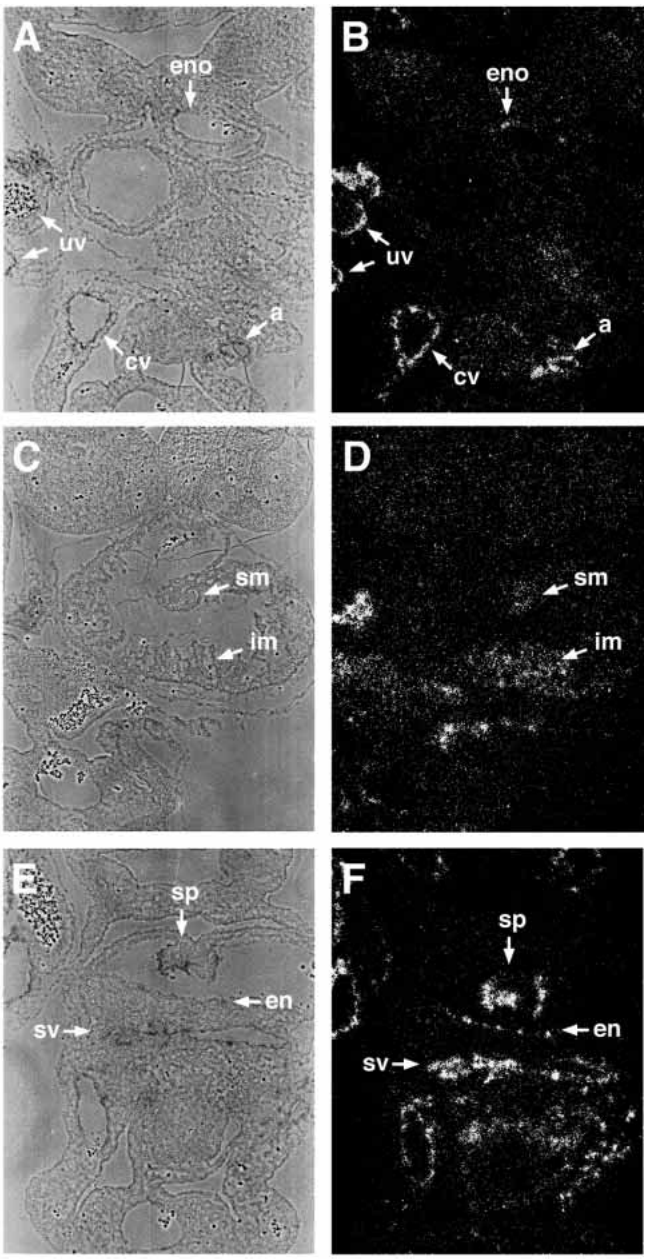

Fig. 6. Expression of *Tll1* in 10.5 dpc mouse embryo hearts. Bright-field (A,C,E) and corresponding dark-field (B,D,F) photomicrographs are shown for in situ hybridization of a *Tll1* antisense probe to transverse sections of a 10.5 dpc embryo heart region. eno, endocardial lining of the outflow tract; a, aorta; cv, cardinal vein; uv, umbilical vein; im and sm, inferior and superior myocardial walls of the common ventricular chamber; sp, septum primum; en, endocardial lining of the common atrial chamber; sv, sinus venosus.

cushion tissue (Fig. 8E,F). Strong expression is also observed in the endocardial lining of the septum primum, and can be seen in the condensed mesenchyme around the trachea, and vasculature, such as the cardinal veins (Fig. 8E,F).

At 13.5 dpc (Fig. 8G), when septation of the left and right ventricles is complete, *Tll1* expression appears to be down-regulated in the MIVS. In contrast, septation of the atria is not complete at this stage (atria are not fully septated until birth) and, correspondingly, strong *Tll1* expression is still present in the septum primum. At 13.5 dpc there also appeared to be some expression in all the endocardial lining of the heart (note punctate expression in trabeculations of the left and right ventricles and lining the atria).

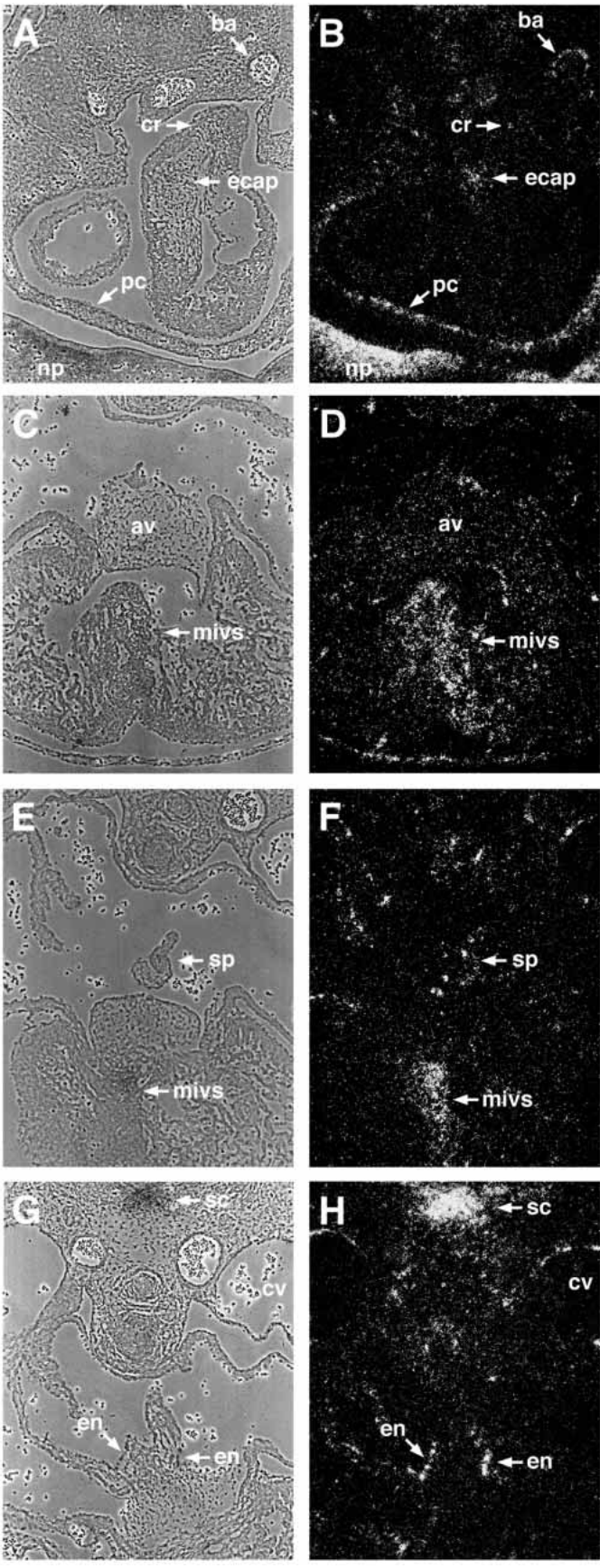

Fig. 7. Expression of *Tll1* in 11.5 dpc mouse embryo hearts. Bright-field (A,C,E,G) and corresponding dark-field (B,D,F,H) photomicrographs are shown for in situ hybridization of a *Tll1* antisense probe to transverse sections of an 11.5 dpc embryo heart. ba, 6th branchial arch artery; cr, cranial ridge of mesenchymatous tissue of aortico-pulmonary spiral septum; ecap, endocardial cushion tissue of aortico-pulmonary septum; pc, pericardium; np, nasal process; mivs, muscular interventricular septum; av, endocardial cushion of the atrio-ventricular canal; sp, septum primum; sc, sclerotomal condensation; cv, cardinal vein; en, endocardial lining adjacent to septum primum.

Differences in the spaciotemporal expression patterns of *Tll1* and *Bmp1* in mouse heart

Proteases BMP-1 and mTLD, encoded by alternatively spliced RNAs of the *Bmp1* gene (Takahara et al., 1994), have substrate specificities which overlap those of mTLL-1 (Scott et al., unpublished data). Thus, since BMP-1 and/or mTLD might compensate for loss of mTLL-1 in tissues in which they are co-expressed, it was of interest to analyze the distributions of the alternatively spliced BMP-1 and mTLD transcripts at selected times in development, for possible expression in heart. At 7.5 and 8.5 dpc, at which times *Tll1* expression is heart-specific (Figs 4, 5), BMP-1 and mTLD RNAs are, in contrast, widely expressed throughout both embryonic and extraembryonic tissues with an almost ubiquitous distribution that appears to overlap the heart-specific expression domain of *Tll1* (Fukagawa et al., 1994; and data not shown). At later developmental stages BMP-1 and mTLD RNAs, while still broadly expressed in mesenchyme, become somewhat more limited in their distributions (Fukagawa et al., 1994; Takahara et al., 1994). At 11.0 and 12.5 dpc BMP-1 and mTLD RNAs are both found at high levels in the atrio-ventricular endocardial cushions (Suzuki et al., 1996 and data not shown), whereas *Tll1* RNA is not detected in this tissue at similar times (see Figs 7, 8; unpublished data). In 12.5 dpc heart, transcripts for BMP-1, mTLD, and mTLL-1 are all expressed at relatively high levels in the endocardial cushion of the aortico-pulmonary septum (Fig. 9). At the same time, however, mTLL-1, but not BMP-1 or mTLD RNA, shows elevated levels of expression specific to the MIVS (Fig. 9).

The only other known mammalian BMP-1/TLD-like protease, the recently discovered mTLL-2, does not share known enzymatic activities with mTLL-1, and its cognate gene, *Tll2*, is not expressed in developing heart, as ascertained by in situ hybridization of normal 7.5 to 13.5 dpc embryos (Scott et al., unpublished data).

Possible mechanisms underlying cardiac defects in Tll1$^{-/-}$ embryos

At the cellular level, TUNEL staining was not increased in *Tll1*$^{-/-}$ MIVS compared to wild type (data not shown), suggesting that failure of the MIVS to fully form results from defects in cellular proliferation and/or differentiation, rather than from an increase in apoptosis. At the molecular level, the most straightforward explanation for the inability of the MIVS to form, and for other cardiac abnormalities in *Tll1*$^{-/-}$ embryos, is insufficient cleavage of mTLL-1 substrate(s) in the absence of this enzyme. Thus far, only two enzymatic activities have been demonstrated for mTLL-1: procollagen C-proteinase activity and the ability to cleave Chordin (Scott et al., unpublished data). In the present study, electron microscopic evaluation showed

normal collagen fibers in the amnion, visceral yolk sac and vena cava of 13.5 dpc *Tll1*$^{-/-}$ embryos, while fibroblasts cultured from 13.5 dpc *Tll1*$^{-/-}$ embryos and analyzed for procollagen processing, as previously described (Suzuki et al., 1996), showed procollagen processing indistinguishable from that of fibroblasts from wild type and heterozygous littermates (data not shown). This is in contrast to results previously obtained with *Bmp1*$^{-/-}$ embryos, in which loss of BMP-1 and mTLD resulted in abnormalities in procollagen processing and fibrillogenesis (Suzuki et al., 1996). Thus, either provision of C-proteinase activity is not a major developmental activity of mTLL-1 (at least in the tissues and cells examined), or loss of mTLL-1 C-proteinase activity is completely compensated for by products of the *Bmp1* gene in *Tll1*$^{-/-}$ embryos. Of particular interest in regard to formation of the MIVS, collagen fibers were not detected by electron microscopy in the MIVS of either *Tll1*$^{-/-}$ or wild-type 13.5 dpc embryos, suggesting that fibrillar collagens do not normally play a role in formation of this structure.

In situ hybridization detected expression of the Chordin gene, *Chrd*, within the hearts of normal 8.5 to 13.5 dpc embryos, at low levels (relative to other tissues such as notochord and developing nerve and cartilage) and not localized to specific structures within the heart (data not shown). To determine the temporal patterns of expression of *Chrd* and *Tll1* in heart and to establish how these might correspond to development of the heart and to each other, RT-PCR was performed on RNA from a developmental series of hearts isolated from normal 8.5-18.5 dpc embryo and adult mice (Fig. 10). In agreement with in situ hybridization results, both *Chrd* and *Tll1* transcripts were present throughout heart development, and were also detected in the adult heart. However, the temporal pattern of expression of *Chrd* was the inverse of that of *Tll1*. Interestingly, at 11.5-13.5 dpc, the period in which *Tll1*$^{-/-}$ cardiac abnormalities become manifest, *Tll1* is expressed at maximum levels and *Chrd* expression is down-regulated.

DISCUSSION

In this study, targeted mutagenesis in ES cells was used to generate mouse embryos homozygous for a disrupted allele at the *Tll1* locus. The resulting phenotype shows that expression of the gene encoding the astacin-like protease mTLL-1 is essential for normal septation and positioning of the mammalian heart and places *Tll1* in a small group of genes whose disruption appears to cause defects confined to the heart. Importantly, the constellation of heart abnormalities constituting the *Tll1*$^{-/-}$ phenotype is unique among cardiac phenotypes of mutant mouse lines reported to date (Rossant, 1996; Fishman and Chien, 1997; de la Pompa et al., 1998; Ranger et al., 1998), thus providing the potential for new insights into heart morphogenesis.

Heart-specific *Tll1* expression in the early embryo and positioning defects of heart and aorta in *Tll1*$^{-/-}$ embryos

It is notable, in light of the heart-specific defects of *Tll1*$^{-/-}$ embryos, that *Tll1* expression in normal early embryos is essentially heart specific. Thus, at 7.5 dpc *Tll1* expression is apparently confined to the heart field of precardiac cells, and at 8.5 dpc embryonic *Tll1* expression is localized to the endocardium of the heart tube. Interestingly, roles have been

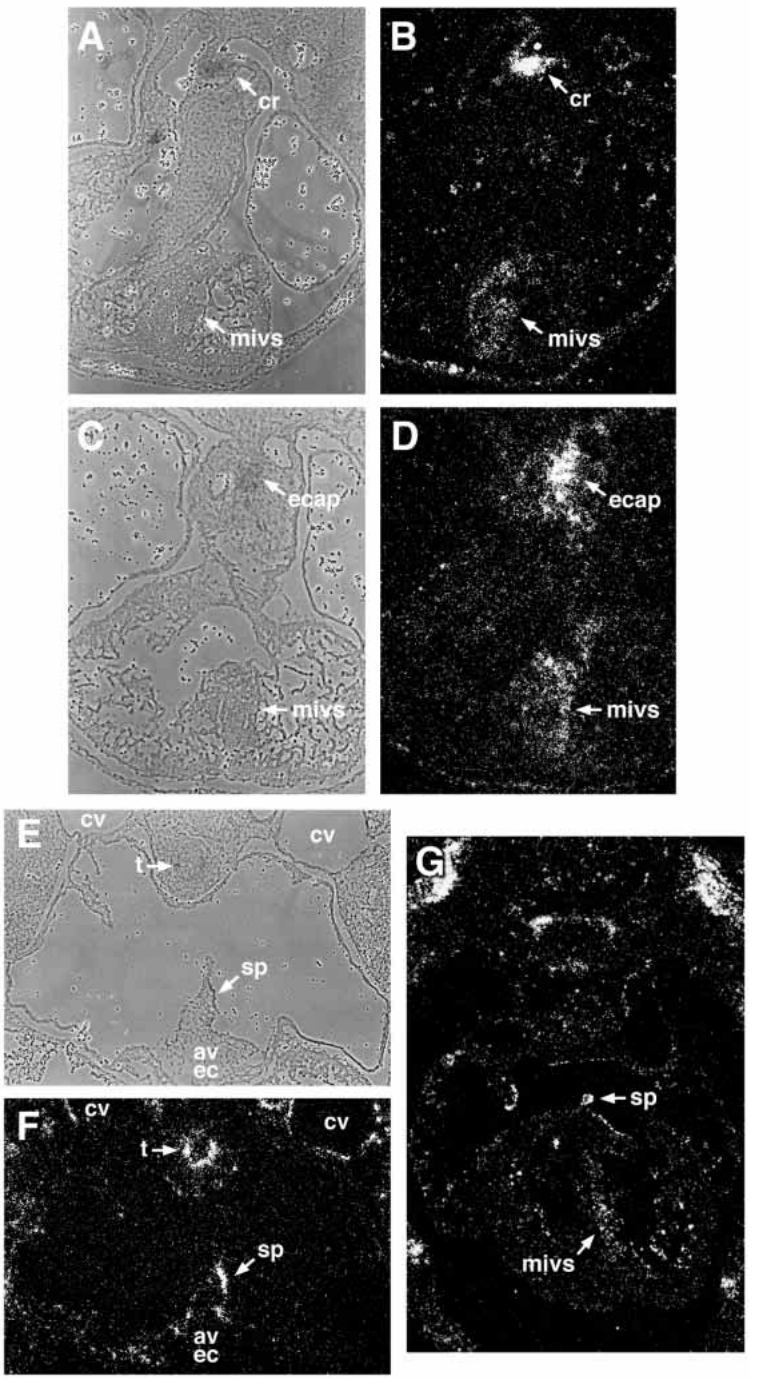

Fig. 8. Expression of *Tll1* in 12.5 dpc mouse embryo hearts. Bright-field (A,C,E) and dark-field (B,D,F,G) photomicrographs are shown for in situ hybridization of a *Tll1* antisense probe to transverse sections of a 12.5 dpc (A-F) and a 13.5 dpc (G) embryo. mivs, muscular interventricular septum; cr, cranial ridge of mesenchymatous tissue of aortico-pulmonary spiral septum; ecap, endocardial cushion of aortico-pulmonary septum; avec, atrio-ventricular endocardial cushion; sp, septum primum; t, trachea; cv, caval veins.

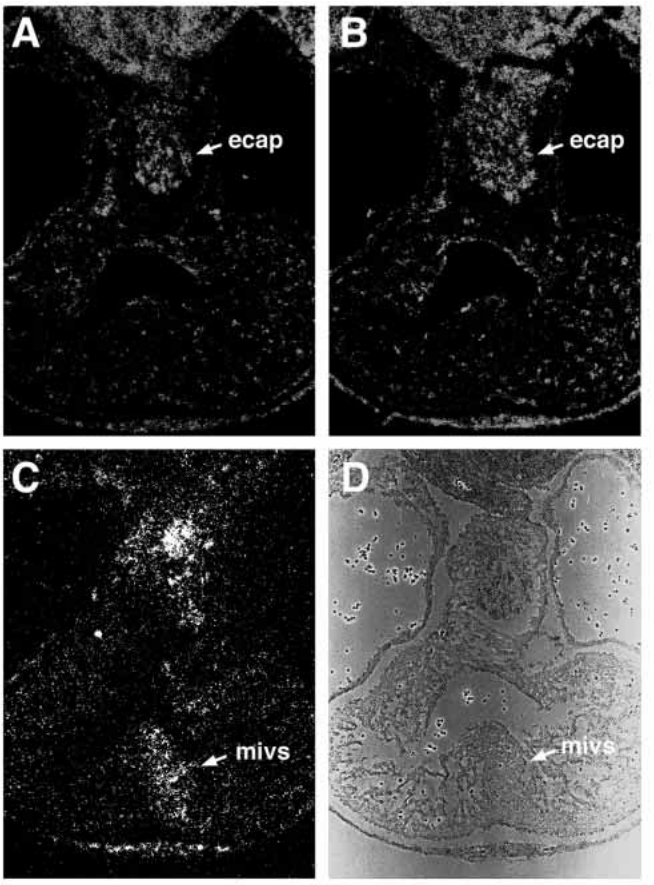

Fig. 9. Expression of mTLD, BMP-1, and mTLL-1 RNAs in serial sections of a 12.5 dpc mouse embryo heart. Dark-field photomicrographs are shown for in situ hybridization of transverse serial sections of a 12.5 dpc heart hybridized to antisense probes specific for mTLD (A) or BMP-1 (B) alternatively spliced RNAs of the *Bmp1* gene, or specific for mTLL-1 RNA of the *Tll1* gene (C). The bright-field photomicrograph corresponding to A is also shown (D).

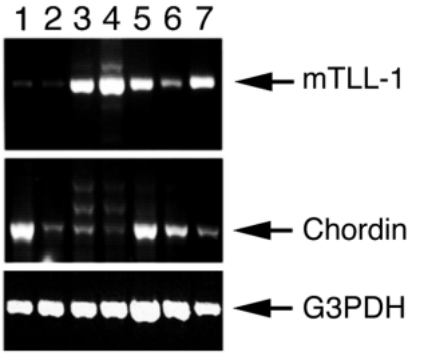

Fig. 10. RT-PCR analysis of RNA encoding mTLL-1 and Chordin in developing and adult mouse hearts. Expression of mTLL-1 (upper panel) or Chordin (middle panel) RNA is detected, by RT-PCR (after 35 cycles of amplification), in isolated 8.5 (lane 1), 9.5 (lane 2), 11.5 (lane 3), 13.5 (lane 4), 15.5 (lane 5), and 18.5 (lane 6) dpc embryo and adult (lane 7) mouse hearts. (Lower panel) Expression of G3PDH (after 27 cycles of amplification) is shown as a control for loading. Each experiment was performed twice with a similar result.

proposed for signaling by TGFβ-like BMPs in formation and maintenance of the heart field in diverse species (Fishman and Chien, 1997; Markwald et al, 1998), while in 8.5 dpc mouse embryos, various BMPs expressed within heart tube myocardium (Lyons et al., 1990; Jones et al., 1991; Lyons et al., 1995; Dudley and Robertson, 1997) are thought to participate in inductive interactions between myocardium and endocardium that influence heart morphogenesis (Fishman and Chien, 1997; Markwald et al., 1998). We have found mTLL-1 to be capable of cleaving Chordin in vitro and of counteracting the dorsalizing effects of Chordin in *Xenopus* embryos (Scott et al., unpublished data), suggesting that mTLL-1, like related proteases (Piccolo et al., 1997; Marqués et al., 1997; Blader et al., 1997), can liberate BMPs from latent BMP/Chordin complexes. Thus, mTLL-1 has the enzymatic activity and is correctly situated to potentiate BMP signaling in the inductive interactions of early heart formation.

A striking observation of the present study was an abnormal and unique positioning of the heart, further left than is normal, and of the descending aorta, to the body midline, in all $Tll1^{-/-}$ embryos examined. In this context, it is of interest that studies of *Bmp2*-null embryos have found that events crucial to normal positioning of the heart may involve BMP signaling within the heart field (Zhang and Bradley, 1996). In zebrafish (Chen et al., 1997), the asymmetric pattern of BMP-4 expression has been shown to drive the lateral asymmetry associated with looping, the process by which, in conjunction with septation, the straight heart tube assumes its mature form and is positioned relative to the left-right axis of the body (Fishman and Chien, 1997; Markwald et al., 1998). Thus, mTLL-1 is necessary to normal positioning of the heart and aorta and may affect these processes through potentiation of BMP signaling in the early stages of heart morphogenesis

At 9.5 dpc, embryonic *Tll1* expression is largely limited to the heart and to the endothelia of blood vessels. In fact, high *Tll1* expression is found at various developmental stages lining embryonic and extraembryonic blood vessels (eg. Figs. 5E,6B,8F), suggesting roles for mTLL-1 throughout the cardiovascular system. From 10.5 dpc onwards, *Tll1* expression is also detected in noncardiovascular tissues such as developing neural tissue and cartilage (Fig. 7H and Takahara et al., 1996). Nevertheless, histological examination of tissues, and ink injection into the hearts of live $Tll1^{-/-}$ embryos for visualization of major vessels (data not shown), found no defects in structures other than heart, perhaps due to functional substitution by *Bmp1* gene products, which are broadly expressed at various developmental stages.

Tll1 and septation

Septation of the primitive mammalian heart tube into the adult four chambered heart is critical for separation of the systemic and pulmonary circulations, required at birth. In the case of the membranous atrial and ventricular septa, and in septation of the AV canals and the aortico-pulmonary channels, this tissue mass is provided by the endocardial cushions (Fishman and Chien, 1997; Markwald et al., 1998). However, the initial septation of common atria and ventricles does not involve the endocardial cushions, but instead involves the ingrowth of myocardial projections: the atrial septum primum and septum secundum, and the muscular portion of the interventricular septum (MIVS) (Webb, et al., 1998; Markwald et al., 1998). Development of

the septa arising from cushion tissue was unaffected in *Tll1*$^{-/-}$ embryos. In contrast, development of the MIVS was defective in all, and development of the atrial muscular septa was defective in most *Tll1*$^{-/-}$ embryos examined. Thus, mTLL-1 is necessary for correct formation of the MIVS and, perhaps, for correct formation of the myocardial atrial septa, as well.

Consistent with the absence of observed defects in AV cushion-derived structures in *Tll1*$^{-/-}$ embryos, *Tll1* expression was not observed in the AV cushions of normal embryos. However, within the outflow tract septum, which forms from a combination of cushion tissue and the influx of cardiac neural crest cells (Conway et al., 1997b; Markwald et al., 1998), *Tll1* is expressed at high levels. This expression appears to be within cells other than neural crest, since levels of *Tll1* expression were unaffected in the neural crest-deficient heart outflow tract of a 13.5 dpc *splotch* embryo (data not shown). Nevertheless, *Bmp1* is also expressed at high levels in the outflow tract septum and, at various developmental stages, within the AV cushions themselves and in attached valve leaflets (unpublished data and Suzuki et al., 1996). Thus, the absence of defects in cushion-derived structures in *Tll1*$^{-/-}$ embryos can be explained by the absence of normal roles for *Tll1* in formation of these structures and/or by functional substitution by *Bmp1*.

In contrast to the AV cushions and outflow tract septum, *Bmp1* is not highly expressed in the developing MIVS, while high *Tll1* expression is associated with this structure throughout its development. Thus, at 9.5 and 10.5 dpc (eg. Fig. 5E) *Tll1* is expressed within the myocardium overlying the apical groove that marks the site where the two ventricular segments fuse as they arise from the heart field, and where the future MIVS will appear (Webb et al., 1997; Markwald et al., 1998). Subsequently, *Tll1* is expressed at high levels in the developing MIVS at 11.5 and 12.5 dpc, subsiding only at 13.5 dpc, at which time septation of the left and right ventricles is complete. Thus, *Tll1* expression correlates well with the initial appearance and subsequent formation of the MIVS and may be a marker for cells involved in this process. Previous morphological observations have suggested that the MIVS might arise from coalescence of trabeculae at the interventricular junction, while, in contrast, in vivo labeling experiments have indicated that the MIVS develops from a single muscular ridge that elevates from the apical junction of the two future ventricles (de la Cruz et al., 1997; Fishman and Chien, 1997; Markwald et al., 1998). If *Tll1* is indeed a marker for MIVS development, then its expression pattern supports the latter process, as high levels of *Tll1* expression are found in the myocardium at the interventricular junction, but not in ventricular trabeculae, even those trabeculae most closely juxtaposed to the forming MIVS.

Twelve of sixteen 13.5 dpc *Tll1*$^{-/-}$ embryos examined, had large openings between left and right atria, while all five 11.0 dpc *Tll1*$^{-/-}$ embryos examined had abnormally large openings between future left and right atria, due to absence of a normal septum primum. Thus, *Tll1* may also be important to interatrial septation. Consistent with this possibility, *Tll1* is expressed at 9.5 dpc in the endocardial lining of the common atrial chamber overlying the future site of the septum primum, and later within the septum primum. However, unlike the developing MIVS, in which *Bmp1* expression is essentially absent, expression of *Bmp1* was observed in the septum primum (data not shown), but at relatively low levels compared to structures such as the outflow septum or AV cushions. Thus, the incomplete penetrance of atrial septation defects in *Tll1*$^{-/-}$ embryos may derive from functional substitution by *Bmp1* in some embryos. However, another possibility is that *Tll1*$^{-/-}$ atrial defects arise secondarily from changes in hemodynamic flow and/or from changes in alignment of atrial structures resulting from primary defects of the MIVS. The appearance of defects such as DORV and DILV in some *Tll1*$^{-/-}$ embryos, also raises the question of whether some component of the observed septation defects may involve misalignment of structures resulting from incomplete looping.

The effects of mTLL-1 protease activity on formation of muscular septa, such as the MIVS, may again involve the potentiation of signaling by BMPs, at least two of which (BMPs 5 and 7) are expressed in developing ventricular myocardium (Dudley and Robertson, 1997). Thus, it is of interest that the temporal patterns of expression for the Chordin and mTLL-1 genes, *Chrd* and *Tll1*, are inversely related in developing heart. In particular, from 11.5 to 13.5 dpc *Tll1* expression in heart is highest and *Chrd* expression is lowest, and it is during this same period that *Tll1*$^{-/-}$ septation defects manifest themselves. Therefore, during this period, BMP signaling may normally be particularly important in the formation of the muscular septa and be maximized in these structures through concomitant down-regulation of inhibitory Chordin and up-regulation of potentiating mTLL-1 molecules. Electron microscopic examination found no evidence for collagen fibrils in wild-type MIVS, making it unlikely that mTLL-1 procollagen C-proteinase activity plays a major role in MIVS formation. Nevertheless, some portion of the cardiac defects in *Tll1*$^{-/-}$ embryos may be due to the failure to process some, as yet unidentified, nonfibrillar matrix substrate(s) of mTLL-1. If so, mTLL-1 may normally influence heart morphogenesis through coordinated effects on the potentiation of TGFβ-like molecules and the deposition of matrix.

Atrial septal defects and defects of the MIVS constitute the most common cardiac abnormalities in humans (Olson and Srivastava, 1996). Thus, identification here of the essential roles of the astacin-like protease mTLL-1 in heart morphogenesis, not only provides new insights into the molecular events underlying formation of the mammalian heart, but has the potential to further our understanding of human cardiovascular disease as well.

We thank Bob Anderson for valuable advice and Guy G. Hoffman, James D. Prahl, and Rhonda Rogers for excellent technical assistance. This work was supported by National Institutes of Health Grants HL60104 and HL60714 (to S. J. C.) and AR43621 and GM46846 (to D. S. G.), by a March of Dimes Basil O'Conner Research Scholar Award (to S. J. C.) and by a grant from FibroGen Inc., South San Francisco, CA. P. A. L. and G. W. were Associates and B. L. M. H. is an Investigator of the Howard Hughes Medical Institute.

REFERENCES

Barnes, W. M. (1994). PCR amplification of up to 35-kb DNA with high fidelity and high yield from bacteriophage templates. *Proc. Natl. Acad. Sci. USA* **91**, 2216-2220.

Beck, E., Ludwig, G., Auerswald, E. A., Reiss, B. and Schaller, H. (1982). Nucleotide sequence and exact localization of the neomycin phosphotransferase gene from transposon Tn5. *Gene* **19**, 327-336.

Blader, P., Rastegar, S., Fischer, N. and Strähle, U. (1997). Cleavage of the BMP-4 antagonist chordin by zebrafish tolloid. *Science* **278**, 1937-1940.

Bond, J. S. and Beynon, R. J. (1995). The astacin family of metalloendopeptidases. *Protein Sci.* **4**, 1247-1261.

Celeste, A. J., Iannazzi, J. A., Taylor, R. C., Hewick, R. M., Rosen, V.,

Wang, E. A. and Wozney, J. M. (1990). Identification of transforming growth factor β family members present in bone-inductive protein purified from bovine bone. *Proc. Natl. Acad. Sci. USA* **87**, 9843-9847.

Chen, J.-N., van Eeden, F. J. M., Warren, K. S., Chin, A., Nüsslein-Volhard, C., Haffter, P. and Fishman, M. C. (1997). Left-right pattern of cardiac BMP4 may drive asymmetry of the heart in zebrafish. *Development* **124**, 4373-4382.

Childs, S. R. and O'Connor, M. B. (1994). Two domains of the tolloid protein contribute to its unusual genetic interaction with decapentaplegic. *Dev. Biol.* **162**, 209-220.

Church, G. M. and Gilbert, W. (1984). Genomic sequencing. *Proc. Natl. Acad. Sci. USA* **81**, 1991-1995.

Conway, S. J., Henderson, D. J., Kirby, M. L., Anderson, R. H. and Copp, A. J. (1997a). Development of a lethal congenital heart defect in the *splotch* (*Pax3*) mutant mouse. *Cardiovascular Res.* **36**, 163-173.

Conway, S. J., Henderson, D. J. and Copp, A. J. (1997b). *Pax3* is required for cardiac neural crest migration in the mouse: evidence from the *(Sp^{2H})* mutant. *Development* **124**, 505-514.

de la Cruz, M. V., Castillo, M. M., Villavicencio, L., Valencia, G. A. and Moreno-Rodriguez, R. A. (1997). Primitive interventricular septum, its primordium, and its
contribution in the definitive interventricular septum: in vivo labelling study in the chick embryo. *Anat. Rec.* **247**, 512-520.

de la Pompa, J. L., Timmerman, L. A., Takimoto, H., Yoshida, H., Elia, A. J., Samper, E., Potter, J., Wakeham, A., Marengere, L., Langille, B. L., Crabtree, G. R. and Mak, T. W. (1998). Role of the NF-ATc transcription factor in morphogenesis of cardiac valves and septum. *Nature* **392**, 182-185.

Downs, K. M. and Davies, T. (1993). Staging of gastrulating mouse embryos by morphological landmarks in the dissecting microscope. *Development* **118**, 1255-1266.

Dudley, A. T. and Robertson, E. J. (1997). Overlapping expression domains of bone morphogenetic protein family members potentially account for limited tissue defects in BMP7 deficient embryos. *Dev. Dyn.* **208**, 349-362.

Finelli, A. L., Bossie, C. A. and Padgett, R. W. (1994). Mutational analysis of the *Drosophila tolloid* gene, a human BMP-1 homolog. *Development* **120**, 861-870.

Fishman, M. C. and Chien, K. R. (1997). Fashioning the vertebrate heart: earliest embryonic decisions. *Development* **124**, 2099-2117.

Fukagawa, M., Suzuki, N., Hogan, B. L. M. and Jones, C. M. (1994). Embryonic expression of mouse bone morphogenetic protein-1 (BMP-1), which is related to the Drosophila dorsoventral gene tolloid and encodes a putative astacin metalloendopeptidase. *Dev. Biol.* **163**, 175-183.

Goodman, S. A., Albano, R., Wardle, F. C., Matthews, G., Tannahill, D. and Dale L. (1998). BMP1-related metalloproteinases promote the development of ventral mesoderm in early Xenopus embryos. *Dev. Biol.* **195**, 144-157.

Hogan, B. L. M., Beddington, R., Costantini, F. and Lacy, E. (1994). *Manipulating the Mouse Embryo: A Laboratory Manual*, Second Edition. Cold Spring Harbor, NY: Cold Spring Harbor Press.

Jones, M., Lyons, K. M. and Hogan, B. L. M. (1991). Involvement of *Bone Morphogenetic Protein-4* (BMP-4) and *Vgr-1* in morphogenesis and neurogenesis in the mouse. *Development* **111**, 531-542.

Kessler, E., Takahara, K., Biniaminov, L., Brusel, M. and Greenspan, D. S. (1996). Bone morphogenetic protein-1: The type I procollagen C-proteinase. *Science* **271**, 360-362.

Komuro, I. and Izumo, S. (1993). Csx: A murine homeobox-containing gene specifically expressed in the developing heart. *Proc Natl. Acad. Sci. USA* **90**, 8145-8149.

Labosky, P. A., Winnier, G. E., Jetton, T. L., Hargett, L., Ryan, A. K., Rosenfeld, M. G., Parlow, A. F. and Hogan, B. L. M. (1997). The winged helix gene, *Mf3*, is required for normal development of the diencephalon and midbrain, postnatal growth and the milk-ejection reflex. *Development* **124**, 1263-1274.

Li, S.-W., Sieron, A. L., Fertala, A., Hojima, Y., Arnold, W. V. and Prockop, D. J. (1996). The C-proteinase that processes procollagens to fibrillar collagens is identical to the protein previously identified as bone morphogenic protein-1. *Proc. Natl. Acad. Sci. USA* **93**, 5127-5130.

Lints, T. J., Parsons, L. M., Hartley, L., Lyons, I. and Harvey, R. P. (1993). Nkx-2.5: a novel murine homeobox gene expressed in early heart progenitor cells and their myogenic descendants. *Development* **119**, 419-431.

Lyons, K. M., Pelton, R. W. and Hogan, B. L. M. (1990). Organogenesis and pattern formation in the mouse: RNA distribution patterns suggest a role for *Bone Morphogenetic Protein-2A* (*BMP-2A*). *Development* **109**, 833-844.

Lyons, K. M., Hogan, B. L. M. and Robertson, E. J. (1995). Colocalization of BMP 7
and BMP 2 RNAs suggests that these factors cooperatively mediate tissue interactions during murine development. *Mech. Dev.* **50**, 71-83.

Markwald, R. R., Trusk, T. and Moreno-Rodriguez, R. (1998). Formation and septation of the tubular heart: Integrating the dynamics of morphology with emerging molecular concepts. In Living Morphogenesis of the Heart (ed. M. V. de la Cruz and R. R. Markwald), pp. 43-84. Boston: Birkhauser (Springer-Verlag).

Marqués, G., Musacchio, M., Shimell, M. J., Wünnenberg-Stapleton, K., Cho, K. W. Y. and O'Connor, M. B. (1997). Production of a DPP activity gradient in the early Drosophila embryo through the opposing actions of the SOG and TLD proteins. *Cell* **91**, 417-426.

Neul, J. L. and Ferguson, E. L. (1998). Spatially restricted activation of the SAX receptor by SCW modulates DPP/TKV signaling in *Drosophila* dorsal-ventral patterning. *Cell* **95**, 483-494.

Nguyen, M., Park, S., Marqués, G. and Arora, K. (1998). Interpretation of a BMP activity gradient in Drosophila embryos depends on synergistic signaling by two type I receptors, SAX and TKV. *Cell* **95**, 495-506.

Olson E. N. and Srivastava, D. (1996). Molecular pathways controlling heart development. *Science* **272**, 671-676.

Panchenko, M. V., Stetler-Stevenson, W. G., Trubetskoy, O. V., Gacheru, S. N. and Kagan, H. M. (1996). Metalloproteinase activity secreted by fibrogenic cells in the processing of prolysyl oxidase. *J. Biol. Chem.* **271**, 7113-7119.

Pappano, W. N., Scott, I. C., Clark, T. G., Eddy, R. L., Shows, T. B. and Greenspan, D. S. (1998). Coding sequence and expression patterns of mouse chordin and mapping of the cognate mouse *Chrd* and human *CHRD* genes. *Genomics* **52**, 236-239.

Piccolo, S., Agius, E., Lu, B., Goodman, S., Dale, L. and De Robertis, E. M. (1997). Cleavage of chordin by xolloid metalloprotease suggests a role for proteolytic processing in the regulation of Spemann organizer activity. *Cell* **91**, 407-416.

Ranger, A. M., Grusby, M. J., Hodge, M. R., Gravallese, E. M., de la Brousse, F. C., Hoey, T., Mickanin, C., Baldwin, H. S. and Glimcher, L. H. (1998). The transcription factor NF-ATc is essential for cardiac valve formation. *Nature* **392**, 186-190.

Rossant, J. (1996). Mouse mutants and cardiac development: New molecular insights into cardiogenesis. *Circ. Res.* **78**, 349-353.

Shimell, M. J., Ferguson, E. L., Childs, S. R. and O'Connor, M. B. (1991). The *Drosophila* dorsal-ventral patterning gene tolloid is related to human bone morphogenetic protein 1. *Cell* **67**, 469-481.

Stöcker, W., Grams, F., Baumann, U., Reinemer, P., Gomis-Rüth, F.-X., McKay, D. B. and Bode, W. (1995). The metzincins – Topological and sequential relations between the astacins, adamalysins, serralysins, and matrixins (collagenases) define a superfamily of zinc-peptidases. *Protein Sci.* **4**, 823-840.

Suzuki, N., Labosky, P. A., Furuta, Y., Hargett, L., Dunn, R., Fogo, A. B., Takahara, K., Peters, D. M. P., Greenspan, D. S. and Hogan, B. L. M. (1996). Failure of ventral body wall closure in mouse embryos lacking a procollagen C-proteinase encoded by *Bmp1*, a mammalian gene related to *Drosophila tolloid*. *Development* **122**, 3587-3595.

Takahara, K., Lyons, G. E. and Greenspan, D. S. (1994). Bone morphogenetic protein-1 and a mammalian tolloid homologue (mTld) are encoded by alternatively spliced transcripts which are differentially expressed in some tissues. *J. Biol. Chem.* **269**, 32572-32578.

Takahara, K., Brevard, R., Hoffman, G. G., Suzuki, N. and Greenspan, D. S. (1996). Characterization of a novel gene product (mammalian tolloid-like) with high sequence similarity to mammalian tolloid/bone morphogenetic protein-1. *Genomics* **34**, 157-165.

Tybulewicz, V. L. J., Crawford, C. E., Jackson, P. K., Bronson, R. T. and Mulligan, R. C. (1991). Neonatal lethality and lymphopenia in mice with a homozygous disruption of the c-abl proto-oncogene. *Cell* **65**, 1153-1163.

Webb, S., Brown, N. A. and Anderson, R. H. (1998). Formation of the atrioventricular septal structures in the normal mouse. *Circ. Res.* **82**, 645-56.

Winnier, G., Blessing, M., Labosky, P. A. and Hogan, B. L. M. (1995). Bone morphogenetic protein-4 is required for mesoderm formation and patterning in the mouse. *Genes Dev.* **9**, 2105-2116.

Wozney, J. M., Rosen, V., Celeste, A. J., Mitsock, L. M., Whitters, M. J., Kriz, R. W., Hewick, R. M. and Wang, E. A. (1988). Novel regulators of bone formation: Molecular clones and activities. *Science* **242**, 1528-1534.

Zhang, H. and Bradley, A. (1996). Mice deficient for BMP2 are nonviable and have defects in amnion/chorion and cardiac development. *Development* **122**, 2977-2986.